GlyR α3: An Essential Target for Spinal PGE_2-Mediated Inflammatory Pain Sensitization

Robert J. Harvey,[1,8]* Ulrike B. Depner,[2]* Heinz Wässle,[3] Seifollah Ahmadi,[2] Cornelia Heindl,[2] Heiko Reinold,[2] Trevor G. Smart,[4] Kirsten Harvey,[1] Burkhard Schütz,[5] Osama M. Abo-Salem,[5] Andreas Zimmer,[5] Pierrick Poisbeau,[6] Hans Welzl,[7] David P. Wolfer,[7] Heinrich Betz,[8]† Hanns Ulrich Zeilhofer,[2] Ulrike Müller[8]†

Prostaglandin E_2 (PGE_2) is a crucial mediator of inflammatory pain sensitization. Here, we demonstrate that inhibition of a specific glycine receptor subtype (GlyR α3) by PGE_2-induced receptor phosphorylation underlies central inflammatory pain sensitization. We show that GlyR α3 is distinctly expressed in superficial layers of the spinal cord dorsal horn. Mice deficient in GlyR α3 not only lack the inhibition of glycinergic neurotransmission by PGE_2 seen in wild-type mice but also show a reduction in pain sensitization induced by spinal PGE_2 injection or peripheral inflammation. Thus, GlyR α3 may provide a previously unrecognized molecular target in pain therapy.

An exaggerated sensation of pain is a cardinal symptom of inflammation. It can result from either increased excitability of primary afferent nociceptive nerve fibers (peripheral sensitization) or changes in the central processing of sensory stimuli (central sensitization) (*1*, *2*). Prostaglandins, namely PGE_2, are key mediators of both central and peripheral pain sensitization (*3*–*5*), and different cellular mechanisms have been proposed for their pronociceptive actions (*6*, *7*). However, their relative contributions in vivo, their precise molecular target(s), and the importance of peripheral versus central sensitization have remained elusive.

We found that the α3 subunit (*8*–*11*) of strychnine-sensitive glycine receptors (GlyRs) (*8*–*11*) is distinctly expressed in the superficial laminae of the mouse dorsal horn (Fig. 1A and fig. S2). Staining consecutive sections with antibodies specific for GlyR α3 (*12*) and calcitonin gene–related peptide (CGRP) showed punctate GlyR α3 immunoreactivity predominantly in lamina II (Fig. 1B), where most nociceptive afferents terminate. All GlyR α3 subunit immunoreactive puncta were found to colocalize with gephyrin (Fig. 1, A and C to E), which clusters GlyRs and $GABA_A$ receptors at postsynaptic sites (*12*). This indicates that α3 GlyRs are synaptic and clustered by gephyrin. Costaining for GlyR α1 subunits [a component of the major GlyR isoform (α1β) in adult spinal cord (*13*)] and α3 subunits revealed 54 ± 3% colocalization (in eight sections, each containing >500 puncta; Fig. 1, F to H, and fig. S1). Thus, both subunit-specific glycinergic synapses (i.e., those that contain either α1 or α3) and mixed glycinergic synapses (those that contain both α1 and α3) exist.

To determine the physiological role of the GlyR α3 subunit, we disrupted the murine gene (*Glra3*) by homologous recombination in embryonic stem (ES) cells (Fig. 2, A to C). Whereas wild-type spinal cord exhibited intense α3 staining (Fig. 2D), no GlyR α3 immunoreactive puncta were detected in $Glra3^{-/-}$ mice (Fig. 2E). Costaining with the GlyR α1 subunit–specific antibody mAb2b (*14*) produced punctate GlyR immunoreactivity in both knockout and wild-type littermates (Fig. 2, F and G, and fig. S1). $Glra3^{-/-}$ mice were obtained at Mendelian frequency and were fertile. They exhibited normal body weight and showed no gross histopathological abnormalities of the brain or spinal cord. A primary behavioral screen of $Glra3^{-/-}$ mice revealed no notable alterations in posture, activity, gait, motor coordination, tremor, or startle response (table S1). Hence, $Glra3^{-/-}$ mice do not display a neuromotor phenotype comparable to that of mice with GlyR mutations in *Glra1* or *Glrb* (*15*–*17*).

The distinct expression of the GlyR α3 subunit in the superficial laminae of the dor-

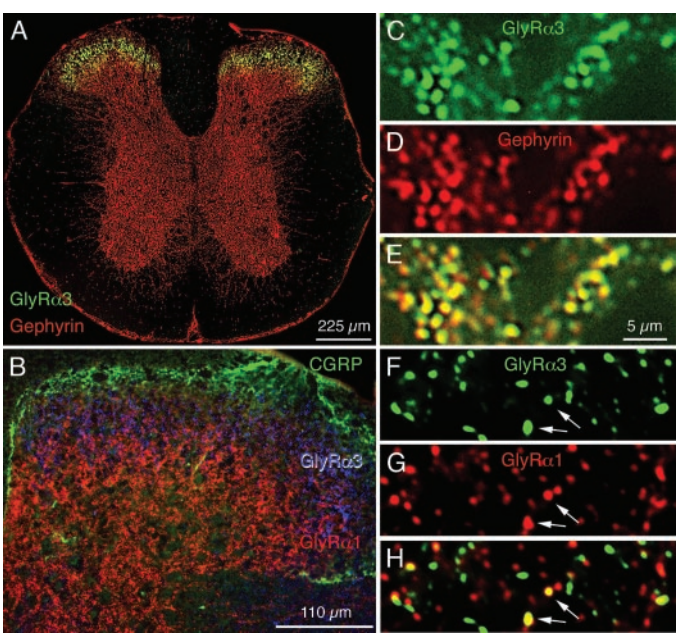

Fig. 1. Colocalization of the GlyR α3 subunit with spinal synaptic markers. Transverse sections through wild-type thoracic spinal cord are shown. (**A**) Double labeling shows that GlyR α3 (green) is restricted to the dorsal horn, and gephyrin (red) is expressed throughout the gray matter. (**B**) Triple immunostaining shows CGRP (green), the GlyR α3 subunit (blue), and the GlyR α1 subunit (red). CGRP immunoreactivity decorates the outer rim (lamina I) of the dorsal horn, whereas GlyR α3 staining is found in lamina II. High-resolution images showing (**C**) 65 GlyR α3–positive puncta and (**D**) 76 gephyrin-immunoreactive puncta. (**E**) Superposition of (C) and (D) reveals a high degree of colocalization. High-resolution images show (**F**) 40 GlyR α3 and (**G**) 57 α1 subunit puncta. (**H**) Superposition of (F) and (G) shows that 21 (54%) of the GlyR α3 puncta coincide with GlyR α1 clusters. The yellow hue is only found in puncta of equal intensity. Arrows in (F) to (H) indicate two colocalized puncta. Details of colocalization analysis are described in the supporting online material.

[1]Department of Pharmacology, The School of Pharmacy, London WC1N 1AX, UK. [2]Institut für Experimentelle und Klinische Pharmakologie und Toxikologie, Universität Erlangen-Nürnberg, D-91054 Erlangen, Germany. [3]Abteilung Neuroanatomie, Max-Planck-Institut für Hirnforschung, D-60528 Frankfurt, Germany. [4]Department of Pharmacology, University College London, London WC1E 6BT, UK. [5]Institut für Molekulare Neurobiologie, Universitätsklinikum Bonn, D-53105 Bonn, Germany. [6]Laboratoire de Neurophysiologie Cellulaire et Intégrée, Université Louis Pasteur/CNRS UMR 7519, 67084 Strasbourg, France. [7]Abteilung für Neuroanatomie und Verhalten, Institut für Anatomie, Universität Zürich–Irchel, CH-8057 Zürich, Switzerland. [8]Abteilung Neurochemie, Max-Planck-Institut für Hirnforschung, D-60528 Frankfurt, Germany.

*These authors contributed equally to this work.
†To whom correspondence should be addressed. E-mail: umueller@mpih-frankfurt.mpg.de (U.M.); neurochemie@mpih-frankfurt.mpg.de (H.B.)

sal horn suggested a role in spinal nociceptive processing (*18*). PGE_2 is known to inhibit glycinergic neurotransmission in the dorsal horn by means of a postsynaptic cyclic adenosine monophosphate–dependent protein kinase (PKA)–mediated pathway (*7*). Therefore, we investigated whether α3 GlyR deficiency would affect PGE_2 modulation of glycinergic neurotransmission (Fig. 3). Am-

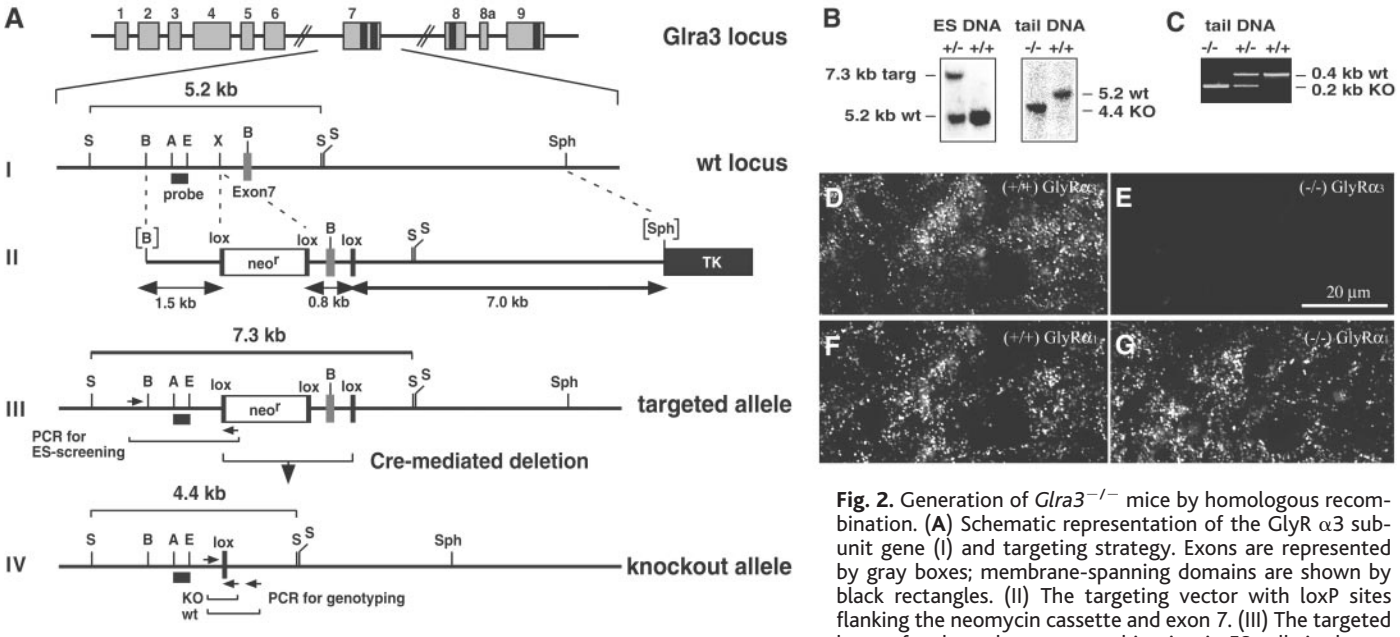

Fig. 2. Generation of *Glra3*$^{-/-}$ mice by homologous recombination. (**A**) Schematic representation of the GlyR α3 subunit gene (I) and targeting strategy. Exons are represented by gray boxes; membrane-spanning domains are shown by black rectangles. (II) The targeting vector with loxP sites flanking the neomycin cassette and exon 7. (III) The targeted locus after homologous recombination in ES cells is shown. Small arrows indicate primers used for polymerase chain reaction (PCR) screening. (IV) *Cre*-mediated recombination removes the neocassette and exon 7. Short arrows indicate primers used for screening of *Cre*-mediated excision and genotyping of animals. A, Ase I; B, Bam HI; E, Eco RV; S, Sac I; X, Xba I; Sph, Sph I; KO, knockout; wt, wild type; TK, thymidine kinase. (**B**) Southern blot of Sac I–cleaved genomic DNA from targeted heterozygous (+/−) and wild-type (+/+) ES cells hybridized with a 380-bp Ase I/Eco RV fragment [labeled "probe" in I of (A)] (left panel). Sac I–cleaved tail DNA of *Glra3*$^{-/-}$ (−/−) and wild-type (+/+) littermates hybridized with the Ase I/Eco RV probe (right panel). (**C**) PCR-genotyping of mice with primers depicted in IV of (A). (**D** to **G**) Fluorescence micrographs of the dorsal horn show immunolabeling for the GlyR α3 and α1 subunits. (D) and (E) show GlyR α3 subunit immunoreactivity in wild-type (+/+) and knockout (−/−) mice. (F) and (G) show GlyR α1 subunit immunoreactivity in wild-type (+/+) and knockout (−/−) mice.

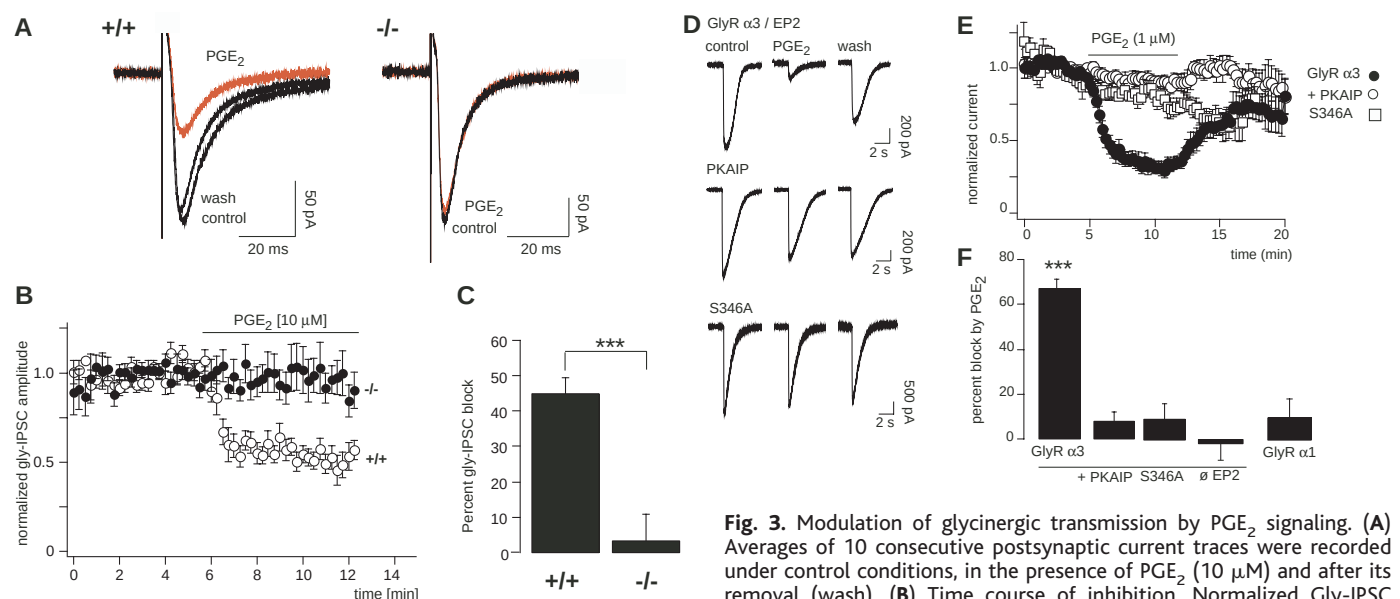

Fig. 3. Modulation of glycinergic transmission by PGE_2 signaling. (**A**) Averages of 10 consecutive postsynaptic current traces were recorded under control conditions, in the presence of PGE_2 (10 µM) and after its removal (wash). (**B**) Time course of inhibition. Normalized Gly-IPSC amplitudes (mean ± SEM) in wild-type (open circles, +/+, $n = 12$) and *Glra3*$^{-/-}$ (closed circles, −/−, $n = 16$) mice are shown. (**C**) Statistical analysis (mean ± SEM) of Gly IPSC inhibition by PGE_2 (10 µM). ***, $P \leq 0.001$, unpaired *t* test. (**D**) Representative glycine-induced current traces in HEK293T cells cotransfected with the GlyR α3L and EP2 receptor cDNAs (top), with 10 µM PKA inhibitor peptide (PKAIP) included in the patch pipette (middle), and after disruption of the PKA consensus sequence Arg-Glu-Ser-Arg within the large intracellular loop of the GlyR α3 subunit by the S346A mutation. (**E**) Time course of inhibition of glycinergic membrane currents through wild-type GlyR α3 (solid circles), mutated GlyR $\alpha3^{S346A}$ (squares), and wild-type GlyR α3 in the presence of PKAIP (open circles). (**F**) Statistical analysis (mean ± SEM) of PGE_2-mediated inhibition of glycinergic membrane currents. ***, $P \leq 0.001$, unpaired *t* test. Upon transfection of the rat GlyR α1 subunit cDNA, no PGE_2-mediated block of glycinergic currents was observed.

plitudes and kinetics of electrically evoked glycinergic inhibitory postsynaptic currents (IPSCs) recorded from spinal cord slices were statistically indistinguishable in wild-type and *Glra3*$^{-/-}$ littermates (supporting online material text). However, bath-applied PGE_2 (10 μM) reversibly reduced the amplitudes of GlyR-mediated IPSCs by ~45% in wild-type mice only; in *Glra3*$^{-/-}$ mice, PGE_2-induced inhibition of glycinergic synaptic transmission was abolished (Fig. 3, A to C, $P < 0.001$).

To characterize the mechanism of α3 GlyR inhibition by PKA, we performed whole-cell recordings from human embryonic kidney (HEK) 293 cells (HEK293T) cells cotransfected with the mouse PGE_2 receptor of the EP2 subtype and the GlyR α3L (L, long; fig. S3) subunit cDNAs (*8*, *10*). Robust membrane currents were activated by short puffer applications of glycine (Fig. 3, D to F). The peak amplitudes of glycine-activated currents were reversibly reduced by bath application of 1 μM PGE_2 (Fig. 3, D to F). This inhibition involved PKA because inclusion of the PKA inhibitor peptide (10 μM) into the patch pipette almost completely prevented PGE_2-mediated depression of glycine-activated currents. Inhibition of α3 GlyRs is likely due to direct receptor phosphorylation, given that mutation $Ser^{346} \rightarrow Ala^{346}$ (S346A) within a strong PKA consensus sequence (residues 344 to 347, Arg-Glu-Ser-Arg in the intracellular loop connecting transmembrane domains 3 and 4) completely abolished the PGE_2-induced effect. Notably, this serine residue is not conserved at the equivalent position of the GlyR α1 subunit (fig. S3). Indeed, no PGE_2-mediated block of glycine-activated currents was observed upon cotransfection of EP2 and GlyR α1 cDNAs (Fig. 3F).

Inactivation of *Glra3* did not affect basal nociception. Under resting conditions, *Glra3*$^{-/-}$ mice and wild-type littermates showed nearly identical thermal and mechanical sensitivities (Fig. 4, A and B, time point = 0 min; fig. S4). However, when injected intrathecally (i.t.) with 0.2 nmol PGE_2 per mouse ($n = 6$ per group), *Glra3*$^{-/-}$ mice exhibited, in contrast to wild-type mice, a complete lack of pain sensitization. Paw withdrawal latencies upon exposure to a defined radiant-heat stimulus (Fig. 4A) and reaction scores upon mechanical stimulation with von-Frey filaments (1 to 100 mN) (Fig. 4, B and C) remained statistically indistinguishable from preinjection values.

This finding allowed us to assess the contribution of PGE_2-mediated inhibition of α3 GlyRs to pain sensitization evoked by peripheral inflammation. Thermal and mechanical nociceptive behavior was monitored after subcutaneous injection of zymosan A or complete Freund's adjuvant (CFA) into the left hind paw of wild-type and *Glra3*$^{-/-}$ mice (Fig. 4, D to G). Both procedures induce spinal COX2 expression and trigger spinal release of PGE_2 (*19*–*21*) but also activate other peripheral and central pain sensitizing pathways [e.g., PGE_2 production in the periphery (*22*) and spinal release of substance P (*23*)]. After the injection of zymosan A, thermal and mechanical pain sensitization developed similarly over the first 4 hours both in wild-type and *Glra3*$^{-/-}$ mice. However, at later stages, starting at 5 hours after the zymosan A injection, *Glra3*$^{-/-}$ mice progressively recovered from sensitization, whereas for wild-type mice, this sensitization remained nearly constant until the end of the observation period (8 hours) (Fig. 4, D and E). This time frame coincides very well with the spinal expression of COX2, which reaches its maximum about 4 to 5 hours after zymosan A injection (*24*). Subcutaneous CFA injection

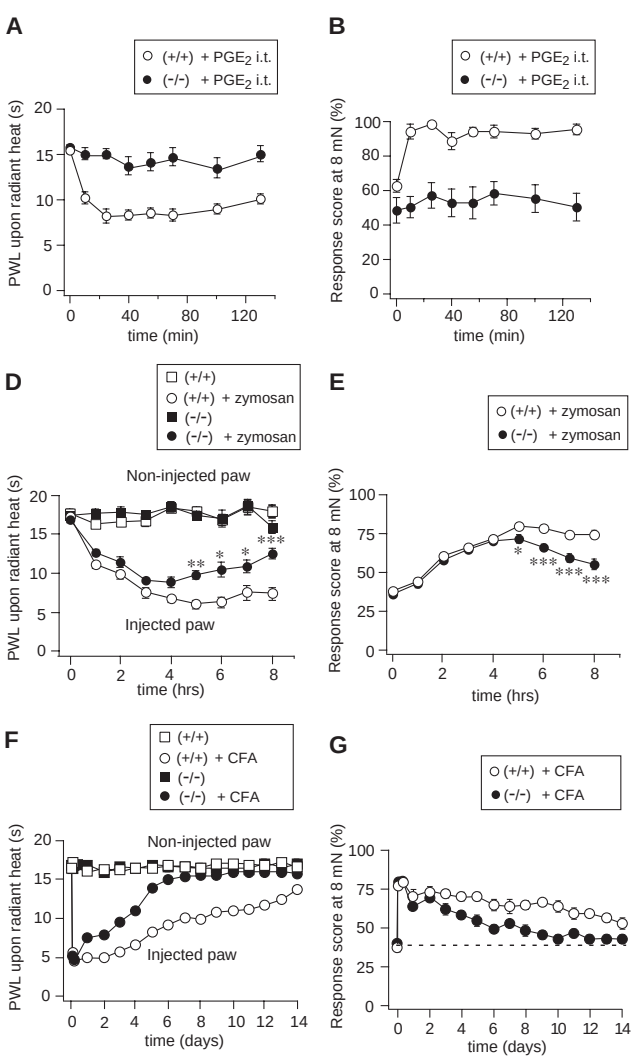

Fig. 4. Pain sensitization induced by intrathecal PGE_2 and peripheral inflammation. (**A** to **C**) Sensitization upon intrathecal (i.t.) PGE_2 injection. (A) Paw withdrawal latencies (PWL, mean ± SEM) of wild-type (open circles) and *Glra3*$^{-/-}$ (solid circles) mice upon exposure to a defined noxious radiant-heat stimulus versus time after intrathecal PGE_2 injection (0.2 nmol per mouse). (B) Response scores (mean ± SEM) of wild-type (open circles) and *Glra3*$^{-/-}$ (solid circles) mice upon mechanical stimulation with an 8-mN von-Frey filament versus time after intrathecal PGE_2 injection. (C) Stimulus-response curves obtained in wild-type (open circles and open triangles) and *Glra3*$^{-/-}$ (solid circles and solid triangles) mice before (open and solid circles) and 40 min after (open and solid triangles) intrathecal injection of PGE_2. Statistical analysis for (A) to (C): In wild-type mice, mechanical and thermal sensitization was significantly different from baseline at all time points [$P \leq 0.001$, based on repeated measures of analysis of variance (ANOVA) followed by Fisher's post-hoc test]. In *Glra3*$^{-/-}$ mice, mechanical sensitization was significantly different from baseline only at 2 mN ($P = 0.042$, based on repeated measures of ANOVA). All other changes remained statistically insignificant ($P \geq 0.22$, $n = 6$ for each). (**D** to **G**) Sensitization upon subcutaneous injection of zymosan A [(D) and (E)] or CFA [(F) and (G)] into one of the hindpaws. [(D) and (F)] Paw withdrawal latencies (PWL) of the injected (open and solid circles) and noninjected (open and solid squares) paw upon exposure to a defined noxious radiant-heat stimulus versus time after subcutaneous zymosan A or CFA injection in wild-type (open circles, +/+) and *Glra3*$^{-/-}$ (solid circles, −/−) mice. [(E) and (G)] Response scores (mean ± SEM) of wild-type (open circles) and *Glra3*$^{-/-}$ (solid circles) mice upon mechanical stimulation with a 8-mN von-Frey filament versus time upon zymosan A or CFA injection. Statistical analysis for (D) to (G): Sensitization induced by zymosan A in *Glra3*$^{-/-}$ mice was significantly different from that observed in wild-type littermates at time points ≥5 hours. *, $P \leq 0.05$; **, $P \leq 0.01$; ***, $P \leq 0.001$, based on repeated measures of ANOVA ($n = 6$ for each). CFA-induced pain sensitization in *Glra3*$^{-/-}$ mice was significantly different from wild-type littermates at the following time points: thermal sensitization, days 1 to 14, $P \leq 0.001$; mechanical sensitization, days 4 to 12, $P \leq 0.05$.

produced a pronounced nociceptive sensitization, which lasted for ≥14 days in wild-type mice (Fig. 4, F and G). In contrast, recovery from sensitization in *Glra3*$^{-/-}$ mice was highly accelerated, already reaching thermal baseline values within 7 days (Fig. 4F). Spinal PGE_2 formation and subsequent reduction of glycinergic inhibition therefore are pivotal processes in central inflammatory pain sensitization.

Our findings demonstrate a unique physiological role for a distinctly expressed GlyR subunit of previously unknown function. Whereas the major spinal GlyR isoform (α1) serves well-established functions in the control of spinal motor circuits, GlyR α3 is selectively involved in spinal nociceptive processing. The localization of α3 GlyRs in the substantia gelatinosa, where primary afferent nociceptive nerve fibers make synaptic connections with projection neurons or interneurons, suggests that the activation of synaptic α3 GlyRs located on the dendrites of these neurons limits the dendritic propagation of excitatory input, similar to what has been described for dendritic $GABA_A$ receptors in the hippocampus (*25*, *26*). Activation of GlyR α3 synapses localized on the somata of these neurons may reduce the generation of output spikes. During inflammatory pain states, PGE_2 disinhibits the spinal transmission of nociceptive input through the spinal cord dorsal horn to higher brain areas through PKA-dependent phosphorylation and inhibition of GlyR α3. This process apparently underlies central thermal and mechanical hypersensitivity, which develops within hours after induction of peripheral inflammation (fig. S5). Pharmacological modulation of GlyR α3 function may thus provide a previously untested and promising strategy for the treatment of pathological pain states.

References and Notes

1. C. J. Woolf, M. W. Salter, *Science* **288**, 1765 (2000).
2. J. Scholz, C. J. Woolf, *Nature Neurosci. Suppl.* **5**, 1062 (2002).
3. H. Vanegas, H. G. Schaible, *Prog. Neurobiol.* **64**, 327 (2001).
4. T. A. Samad, A. Sapirstein, C. J. Woolf, *Trends Mol. Med.* **8**, 390 (2002).
5. A. B. Malmberg, T. L. Yaksh, *Science* **257**, 1276 (1992).
6. H. Baba, T. Kohno, K. A. Moore, C. J. Woolf, *J. Neurosci.* **21**, 1750 (2001).
7. S. Ahmadi, S. Lippross, W. L. Neuhuber, H. U. Zeilhofer, *Nature Neurosci.* **5**, 34 (2002).
8. J. Kuhse, V. Schmieden, H. Betz, *J. Biol. Chem.* **265**, 22317 (1990).
9. M. L. Malosio *et al.*, *J. Biol. Chem.* **266**, 2048 (1991).
10. Z. Nikolic *et al.*, *J. Biol. Chem.* **273**, 19708 (1998).
11. S. Haverkamp *et al.*, *J. Comp. Neurol.* **465**, 524 (2003).
12. G. Feng *et al.*, *Science* **282**, 1321 (1998).
13. C.-M. Becker, W. Hoch, H. Betz, *EMBO J.* **7**, 3717 (1998).
14. S. Schröder, W. Hoch, C.-M. Becker, G. Grenningloh, H. Betz, *Biochemistry* **30**, 42 (1991).
15. S. F. Kingsmore *et al.*, *Nature Genet.* **7**, 136 (1994).
16. S. G. Ryan *et al.*, *Nature Genet.* **7**, 131 (1994).
17. M. S. Buckwalter, S. A. Cook, M. T. Davisson, W. F. White, S. A. Camper, *Hum. Mol. Genet.* **3**, 2025 (1994).
18. T. P. Doubell, R. T. Mannion, C. J. Woolf, *The Textbook of Pain*, P. D. Wall, R. Melzack, Eds. (Churchill Livingstone, Edinburgh, ed. 4, 1999), pp. 165–182.
19. F. Beiche, S. Scheuerer, K. Brune, G. Geisslinger, M. Goppelt-Struebe, *FEBS Lett.* **390**, 165 (1996).
20. C. Maihöfner *et al.*, *Neuroscience* **101**, 1093 (2000).
21. T. A. Samad *et al.*, *Nature* **410**, 471 (2001).
22. N. S. Doherty, T. H. Beaver, K. Y. Chan, J. E. Coutant, G. L. Westrich, *Br. J. Pharmacol.* **91**, 39 (1987).
23. M. E. Turnbach, A. Randich, *Pain* **97**, 127 (2002).
24. H. Gühring *et al.*, *J. Neurosci.* **20**, 6714 (2000).
25. R. Miles, K. Toth, A. I. Gulyas, N. Hajos, T. M. Freund, *Neuron* **16**, 815 (1996).
26. R. Cossart *et al.*, *Nature Neurosci.* **4**, 52 (2001).

27. Supported by Max-Planck-Gesellschaft, Bundesministerium für Bildung und Forschung, and Fonds der Chemischen Industrie (H.B. and U.M.), Deutsche Forschungsgemeinschaft Ze 377/6-1 and 377/7-1 (H.U.Z.), Swiss National Science Foundation (D.P.W.) and the Medical Research Council (R.J.H. and T.G.S.). We thank N. Fürst, E. Löwen, B. Layh, and R. Lang for technical assistance, M. Baier for help with preparation of the manuscript, and F. Nyberg (Uppsala, Sweden) for the CGRP antibody, and S. Narumiya (Kyoto, Japan) for the EP2 receptor cDNA clone.

Supporting Online Material

www.sciencemag.org/cgi/content/full/304/5672/884/DC1
Materials and Methods
SOM Text
Figs. S1 to S5
Table S1
References and Notes

19 December 2003; accepted 2 April 2004